

Propagation of femtosecond laser radiation through cloud aerosol: Monte Carlo simulation

Yu.E. Geints, A.A. Zemlyanov, G.M. Krekov,
M.M. Krekova, and G.G. Matvienko

*Institute of Atmospheric Optics,
Siberian Branch of the Russian Academy of Sciences, Tomsk*

Received May 11, 2006

We present preliminary results of a numerical solution (by the Monte Carlo method) of the nonstationary radiation transfer equation for the case of an optically dense disperse medium. As a model medium, we took a homogeneous water droplet cloud. It is expected that an ultra short (about 50-fs duration) intense laser pulse stimulates nonstationary transient process inside the volume of a scattering particle. The result can be transformation in time of its optical characteristics and, primarily, of its scattering phase function. To calculate the dynamics of the scattering phase function of a transparent spherical particle, the nonstationary Mie theory was used, based on the Fourier transform of the initial light pulse and the linear theory of radiation diffraction on a sphere. The field scattered by a particle and the internal field inside the particle are written in the form of the integral of convolution of the pulse spectrum with the spectral response of the particle. Based on spatiotemporal diagrams of light intensity, we have isolated four stages in the nonstationary light scattering by a particle. Then the calculated optical characteristics of a particle have been used as input parameters in solving the problem on multiple scattering of the light pulse by a water aerosol.

Introduction

One of the specific features of a pulsed radiation of ultra-short duration is its broadbandness. The spectral width $\Delta\omega$ of a pulse is inversely proportional to the pulse duration t_p and can make the values $\Delta\omega_p \sim 10^{15} - 10^{16}$ Hz at $t_p \approx 10^{-14} - 10^{-15}$ s. Such a wide frequency range enables simultaneous excitation in a particle of a large number of high-Q electromagnetic vibrational eigenmodes, the whispering gallery modes (WG), the existence of which was recorded experimentally and then proved theoretically.^{1,2} When the frequency of the optical wave incident on a particle coincides with the frequency of one of the particle's eigenmodes, there occurs resonance excitation of the internal optical field. The spatiotemporal distribution of this field is entirely determined by the morphology of the excited mode. Typical lifetimes τ_R of the highest quality WG modes in micron-sized particles are, as a rule, about nanoseconds. Thus, if the duration of the original pulse is comparable with or less than τ_R , then its scattering by a particle can become non-stationary.

1. Single scattering of a femtosecond-duration radiation by a microparticle

The problem of femtosecond pulse scattering by a microparticle belongs to the problems of diffraction of non-stationary and, generally, inhomogeneous optical field on a dielectric sphere. Traditionally it is solved using the approach that combines the spectral

Fourier method with the linear Mie theory. The initial non-stationary problem of diffraction is in this case reduced to the stationary problem of scattering of a set of monochromatic Fourier harmonics by a spherical particle. Here, the scattering properties of a particle are characterized by the so-called spectral response function $\mathbf{E}_s(\mathbf{r}; \omega)$, which is a traditional Mie series written for all the frequencies of the initial pulse spectrum.³ A detailed description of this technique with details of its numerical realization can be found in Refs. 4 and 5. Here we restrict ourselves to summary of the main expressions.

In the numerical calculations, we used the following representation of the electric field strength of the incident linearly polarized radiation:

$$\begin{aligned} \mathcal{E}^i(\mathbf{r}; t) &= \frac{1}{2} \left[\mathbf{E}^i(\mathbf{r}; t) + (\mathbf{E}^i(\mathbf{r}; t))^* \right] = \\ &= \frac{1}{2} E_0 \mathbf{e}_y g(t) S(\mathbf{r}_\perp) \exp[i\omega_0(t - (z + a_0)/c)] + \text{c.c.}, \quad (1) \end{aligned}$$

where $g(t)$ and $S(\mathbf{r}_\perp)$ are the temporal and spatial profiles of the pulse, respectively; ω_0 is the carrier frequency of the pulse; E_0 is the real field amplitude; $\mathbf{r} = \mathbf{r}_\perp + \mathbf{e}_z z$; $\mathbf{r}_\perp = \mathbf{e}_x x + \mathbf{e}_y y$; $\mathbf{e}_x, \mathbf{e}_y, \mathbf{e}_z$ are the unit vectors along the x, y , and z axes, respectively; t is the time; c is the speed of light in vacuum. We assumed that a dielectric spherical particle with the radius a_0 was placed at the origin of coordinates, and the laser pulse diffracting on it propagated along the positive direction of the z axis. The temporal and spatial profiles of the optical signal were specified by the Gaussian functions

$$g(t) = \exp\left\{-\frac{(t - (z + a_0)/c - t_0)^2}{t_p^2}\right\};$$

$$S(\mathbf{r}_\perp) = \exp\left\{-\frac{(x^2 + y^2)}{w_0^2}\right\} \quad (2)$$

with the following parameters: t_p and t_0 are the pulse duration and time delay; w_0 is the spatial half-width of the beam.

The first step in solving this problem is transition from time coordinates to the spectral frequencies using the Fourier representation of the original optical pulse $G(\omega)$:

$$\mathbf{E}_\omega^i(\mathbf{r}, \omega) = \mathfrak{F}[\mathbf{E}^i(\mathbf{r}, t)] =$$

$$= \frac{1}{2} E_0 \mathbf{e}_y S(\mathbf{r}_\perp) G(\omega - \omega_0) e^{-ik_0(z+a_0)}, \quad (3)$$

where \mathfrak{F} is the Fourier transform operator; $k_0 = \omega_0/c$.

Equation (3) multiplied by the exponent $e^{i\omega t}$ determines the spectral component of the initial pulse as a monochromatic wave with the partial amplitude

$$\mathbf{A}(\omega) = E_0 \mathbf{e}_y S(\mathbf{r}_\perp) G(\omega - \omega_0). \quad (4)$$

Diffraction of this wave on a spherical particle is described within the stationary approximation of the Maxwell equations:

$$\text{rot} \mathbf{E}_\omega(\mathbf{r}; \omega) = -ik \mathbf{H}_\omega(\mathbf{r}; \omega);$$

$$\text{rot} \mathbf{H}_\omega(\mathbf{r}; \omega) = i\epsilon_a k \mathbf{E}_\omega(\mathbf{r}; \omega), \quad (5)$$

where $\mathbf{H}_\omega(\mathbf{r}; \omega)$ is the vector of magnetic field strength; ϵ_a is the complex dielectric constant of the particulate matter; $k = \omega/c$. The boundary conditions on the spherical particle surface ($r = |\mathbf{r}| = a_0$) are set based on the requirement that tangential components \mathbf{E}_ω and \mathbf{H}_ω of the internal field keep continuity in crossing the particle surface:

$$[\mathbf{E}_\omega \times \mathbf{n}_r] = [(\mathbf{E}_\omega^i + \mathbf{E}_\omega^s) \times \mathbf{n}_r];$$

$$[\mathbf{H}_\omega \times \mathbf{n}_r] = [(\mathbf{H}_\omega^i + \mathbf{H}_\omega^s) \times \mathbf{n}_r], \quad (6)$$

where \mathbf{n}_r is the vector of the external normal with respect to the particle surface; the superscript s refers to the field of a scattered wave.

Solution of Eq. (5) taking into account Eqs. (4) and (6), with the spatial beam profile set as the Gaussian function (2), gives the following spectral representation of the electric field of an optical wave scattered by a particle:

$$\mathbf{E}_\omega^s(\mathbf{r}; \omega) = E_0 G(\omega - \omega_0) \times$$

$$\times \sum_{n=1}^{\infty} \sum_{m=-n}^n R_n \left[a_{nm}(m_a k a_0) \mathbf{M}_{nm}^{(3)}(kr, \theta, \varphi) - \right.$$

$$\left. - i b_{nm}(m_a k a_0) \mathbf{N}_{nm}^{(3)}(kr, \theta, \varphi) \right], \quad (7)$$

where

$$R_n = i^n \frac{2n+1}{n(n+1)};$$

$\mathbf{M}_{nm}^{(3)}$ and $\mathbf{N}_{nm}^{(3)}$ are the spherical vector-harmonics; m_a is the index of complex refraction of particle substance. The generalized coefficients a_{nm} and b_{nm} are connected with the Mie coefficients for a plane wave a_n and b_n (these notations were introduced in Ref. 6) by the following expressions:

$$a_{nm} = b_n (g_{nm})_{\text{TH}}, \quad b_{nm} = b_n (g_{nm})_{\text{TE}},$$

where $(g_{nm})_{\text{TH}}$ and $(g_{nm})_{\text{TE}}$ are the beam shape coefficients (BSC) being double integrals of the original beam's radial field components.⁷⁻¹⁰ For a weakly focused Gaussian beam (2) centered at the z axis they have the form:

$$(g_{nm})_{\text{TH}} = \frac{1}{2} (-is)^{|m|-1} \exp\left\{-\left(\xi_0^2 + \eta_0^2\right)\right\} \frac{(\xi_0 - i\eta_0)^{|m|-1}}{(m-1)!};$$

$$(g_{nm}(\xi_0, \eta_0))_{\text{TE}} = (-i)^m (g_{nm}(\eta_0, -\xi_0))_{\text{TH}}, \quad m \geq 0;$$

$$(g_{n(-m)}(\xi_0, \eta_0))_{\text{TE}} = -(g_{nm}(\xi_0, -\eta_0))_{\text{TE}},$$

where $\xi_0 = x_0/w_0$ and $\eta_0 = y_0/w_0$ are the dimensionless coordinates of beam's focal waste center (x_0, y_0) ; $s = 1/(k_0 w_0)$ is a dimensionless parameter. For a plane wave linearly polarized along the y axis, all the BSC equal zero, except $(g_{n(\pm 1)})_{\text{TE}} = 1/2$ and $(g_{n(\pm 1)})_{\text{TH}} = \mp(i/2)$. Within the considered approach, the electric field of the optical wave scattered by a particle is presented as an integral of convolution of the initial pulse spectrum with the function of spectral response of the particle:

$$\mathbf{E}(\mathbf{r}; t) = E_0 \mathfrak{F}^{-1} [G(\omega - \omega_0) \mathbf{E}_\omega^s(\mathbf{r}; \omega)]. \quad (8)$$

Here, $\mathbf{E}_\omega^s(\mathbf{r}; \omega)$ stands for the series in the right-hand part of Eq. (7). From Eq. (8) the expression follows for the scattering intensity of a short optical pulse by a spherical particle:

$$I_s(r, \theta, \varphi; t) = I_0 \sum_{n=1}^{\infty} \sum_{m=-n}^n \left\{ \left| a_{nm}(m_a a_0; t) \tilde{\mathbf{M}}_{nm}^{(3)}(\theta, \varphi) \right|^2 + \right.$$

$$\left. + \left| b_{nm}(m_a a_0; t) \tilde{\mathbf{N}}_{nm}^{(3)}(\theta, \varphi) \right|^2 \right\}, \quad (9)$$

where $\tilde{\mathbf{M}}_{nm}^{(3)}$ and $\tilde{\mathbf{N}}_{nm}^{(3)}$ are referred to as the angular part of the spherical harmonics. The time-dependent expansion coefficients $a_{nm}(m_a a_0; t)$ and $b_{nm}(m_a a_0; t)$ are determined by the following expressions:

$$a_{nm}(m_a a_0; t) = \mathfrak{F}^{-1} \left[G(\omega - \omega_0) \hat{\mathbf{M}}_{nm}^{(3)}(kr) a_{nm}(m_a k a_0) \right]; \quad (10)$$

$$b_{nm}(m_a a_0; t) = \mathfrak{F}^{-1} \left[G(\omega - \omega_0) \hat{\mathbf{N}}_{nm}^{(3)}(kr) b_{nm}(m_a k a_0) \right]. \quad (11)$$

Here, $\hat{\mathbf{M}}_{nm}^{(3)}$ and $\hat{\mathbf{N}}_{nm}^{(3)}$ belong to the radial part of the spherical harmonics.

2. Characteristics of nonstationary elastic scattering

In our numerical modeling, the complex particle refraction index m_a and the laser radiation wavelength λ_0 are assumed to be $m_a = 1.33 - i \cdot 10^{-8}$; $\lambda_0 = 0.8 \mu\text{m}$, which corresponds, for example, to water molecules exposed to Ti:Sapphire laser pulses. The frequency dispersion of the particle refractive index in the chosen wavelength range is neglected, also neglected are the nonlinear optical effects of multiphoton ionization and multiphoton absorption.

Time behavior of the optical field scattered by a water droplet exposed to a laser pulse with the plane wave front is illustrated in Fig. 1. For clarity, all the intensity values in Fig. 1 are normalized to their maximum values in the considered spatial region ($r = 100a_0$). The origin of the time axis is the moment when the leading edge of the pulse front (at the level of e^{-2} of the intensity maximum) penetrates into the particle.

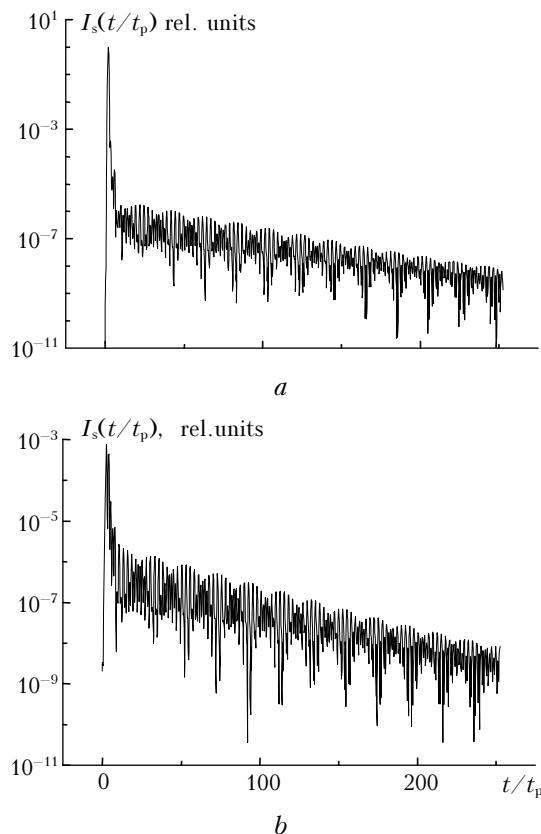


Fig. 1. Time behavior of the relative intensity of radiation scattered forward ($\theta = 0^\circ$) (a) and backward ($\theta = 180^\circ$) (b) from a water droplet with $a_0 = 5 \mu\text{m}$ for the case of laser pulse with $t_p = 50 \text{ fs}$ and $t_0 = 2t_p$.

Maximal volume values of the spectral response function of a water droplet $E_s^{\text{max}}(\omega)$ depending on the relative frequency shift from the central radiation frequency $\Delta\bar{\omega} = (\omega - \omega_0)/\omega_0$ are shown in Fig. 2.

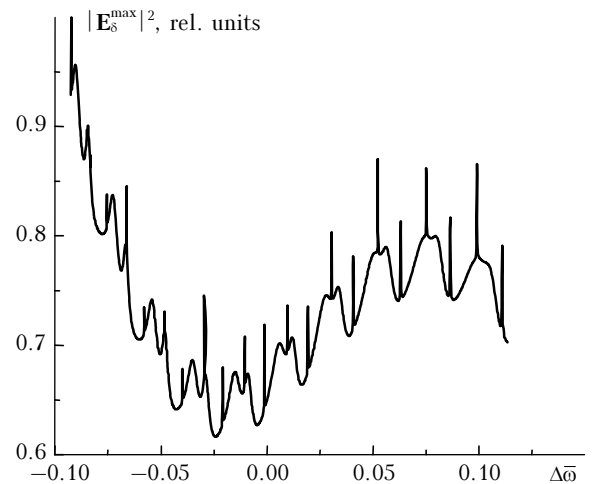


Fig. 2. Spectral behavior of the maximal volume values of the water droplet response function with $a_0 = 5 \mu\text{m}$ for radiation with $\lambda_0 = 0.8 \mu\text{m}$.

From these figures we can see that the time dependence of the optical field intensity is generally characterized by two patterns: the pattern that practically reproduces the time profile of incident radiation and a tail that exponentially falls off with time. This “afterglow” results from the delay of the incident wave field by high-Q WG modes in the particle. Their effective simultaneous excitation occurs owing to a broad frequency spectrum of the laser pulse (see Fig. 2). Time duration of the “afterglow” phase can be large and can make, depending on time parameters, tens and hundreds of lengths of the original pulse. Besides, at this stage one can observe large-scale periodic intensity pulsations, having the features of the frequency beatings among several most high-Q resonance modes stuffed with the high-frequency background.

The normalized scattering phase function of a water droplet $\bar{I}_s(\theta)$ in the femtosecond pulse field is depicted in Fig. 3.

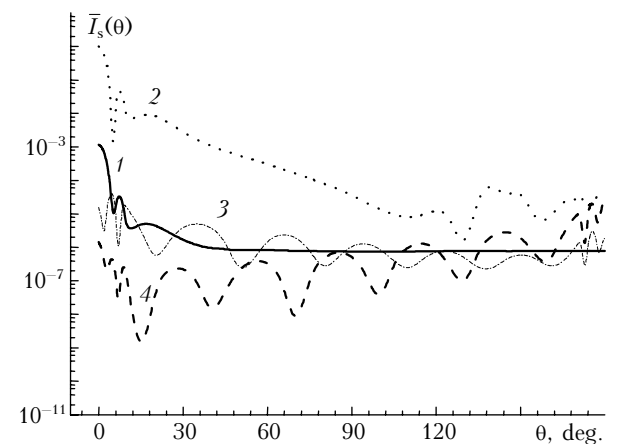


Fig. 3. The scattering phase function of a water droplet with $a_0 = 5 \mu\text{m}$ exposed to a laser pulse with $t_p = 50 \text{ fs}$, $t_0 = 2t_p$ at different time moments $\bar{t} = t/t_p = 1$ (1), 2 (2), 10 (3), and 20 (4).

In this figure, one can see four time stages in the formation the scattering phase function that correspond to three conditional phases of the scattering process, namely, 1) the moment of in-particle penetration of ~10% of the initial pulse energy (curve 1), 2) scattering of a half of the pulse energy (curve 2), and 3) the moment at which the pulse completely leaves the particle (curves 3 and 4). One can see that the shape of the scattering phase function is different in each of the three phases. The first two phases give the most of the forward scattering, which is typical of the usual stationary light scattering by an optically large particle (the diffraction parameter of a five-micron droplet for a 0.8 μm wavelength is ~39). Note that the entire first phase (curve 1) features almost no visible backscattering. It appears only in the end of the second phase (curve 2). The third phase has alternating forward and backward scattering peaks with gradual reduction of their amplitude, which corresponds to pulsations in emission at the resonance modes of the particle, which have accumulated a part of the pulse energy.

3. Multiple scattering of femtosecond radiation in a liquid-droplet cloud

Calculated characteristics of nonstationary elastic scattering at a single droplet make the basis for formulation and solution of the problem of femtosecond radiation transfer in a finite volume of a liquid-droplet cloud medium. Formally, this implies solution of the nonstationary transfer equation with a time-dependent kernel. This is not a trivial problem. Our first numerical estimates can be found in Ref. 11, where we have numerically studied spatiotemporal development of the optical field around the channel of high-power laser radiation that vaporizes the liquid-droplet aerosol along the propagation path. The calculations were based on the algorithm, where we combined the Monte Carlo method with the discrete ordinates method. In the current calculations, we follow the technique used in Ref. 11. The natural basis for discretization of nonstationary transformation of the scattering phase function is the above phases of the optical field evolution inside a particle. Thus, we consider the nonstationary integro-differential Boltzmann equation in a 3D space $\mathbf{r} = \mathbf{r}(x, y, z)$:

$$\begin{aligned} v^{-1} \frac{\partial I(\mathbf{r}, \boldsymbol{\omega}, t, \lambda)}{\partial t} + \boldsymbol{\omega} \nabla I(\mathbf{r}, \boldsymbol{\omega}, t, \lambda) = \\ = -\sigma(\mathbf{r}, t, \lambda) I(\mathbf{r}, \boldsymbol{\omega}, t, \lambda) + \frac{1}{4\pi} \int_{\Lambda} \int_{2\pi} I(\mathbf{r}, \boldsymbol{\omega}', t, \lambda') \times \\ \times \int_t^{t^*} G(\mathbf{r}, \boldsymbol{\omega}', \boldsymbol{\omega}, t', \lambda') dt' d\boldsymbol{\omega}' d\lambda' + I_0(\mathbf{r}, \boldsymbol{\omega}, t, \lambda); \quad (12) \end{aligned}$$

$$\begin{aligned} G(\mathbf{r}, \boldsymbol{\omega}', \boldsymbol{\omega}, t, \lambda) = \\ = G_M(\mathbf{r}, \boldsymbol{\omega}', \boldsymbol{\omega}, t, \lambda' = \lambda) + \int_{\Lambda} G_R(\mathbf{r}, \boldsymbol{\omega}', \boldsymbol{\omega}, t, \lambda') d\lambda', \quad (13) \end{aligned}$$

where $I(\mathbf{r}, \boldsymbol{\omega}, t, \lambda)$ stands for the intensity of radiation with the wavelength λ at the point \mathbf{r} propagating along the $\boldsymbol{\omega}(a, b, c)$ direction at the time moment t ; $I_0(\mathbf{r}, \boldsymbol{\omega}, t, \lambda)$ is the source function (see, for example, Ref. 12); v is the absolute value of the speed of particle motion in the medium,

$$\mathbf{v} = v\boldsymbol{\omega}, \quad \boldsymbol{\omega} = \boldsymbol{\omega}(a, b, c), \quad a^2 + b^2 + c^2 = 1;$$

$G_M(\mathbf{r}, \boldsymbol{\omega}', \boldsymbol{\omega}, t, \lambda' = \lambda)$ is the volume coefficient of directional monochromatic elastic scattering (Mie scattering) along the direction $\boldsymbol{\vartheta} = \boldsymbol{\omega}'\boldsymbol{\omega}$; $G_R(\mathbf{r}, \boldsymbol{\omega}', \boldsymbol{\omega}, t, \lambda')$, is the same for broadband elastic and inelastic (in particular, Raman) scattering; $\sigma(\mathbf{r}, t, \lambda) = \sigma_a(\mathbf{r}, t, \lambda) + \sigma_s(\mathbf{r}, t, \lambda)$ is the extinction coefficient; σ_a, σ_s are the coefficients of absorption and scattering, respectively.

At this stage we use a series of simplifying assumptions. First, we neglect the effects of frequency redistribution of radiation, i.e., we assume $G_R = 0$; second, we believe that the process of interaction of the femtosecond pulse with the droplet is characterized by changes only in the scattering phase function. Therefore,

$$\sigma(\mathbf{r}, t, \lambda) = \sigma(\mathbf{r});$$

$$G(\mathbf{r}, \boldsymbol{\omega}', \boldsymbol{\omega}, t, \lambda) = \sigma_s(r)g(\boldsymbol{\mu}, t),$$

where $g(\boldsymbol{\mu}, t)$ is the normalized scattering phase function;

$$\int_{-1}^1 g(\boldsymbol{\mu}, t) d\boldsymbol{\mu} = 1, \quad \boldsymbol{\mu} = \boldsymbol{\omega}' \cdot \boldsymbol{\omega}.$$

For semi-infinite scattering media (Ref. 12), the Monte Carlo method is ineffective. Usually (see, e.g., Ref. 13), it is assumed that the space Q , where the radiation is transferred, is confined by some convex surface Γ and $\sigma(\mathbf{r}, t, \lambda) \geq \sigma_m > 0$ at $\mathbf{r} \in Q$.

Then, the natural boundary conditions for Eq. (12) have the form

$$I(\mathbf{r}, \boldsymbol{\omega}, t, \lambda) = 0, \quad \text{if } \mathbf{r} \in \Gamma \text{ and } (\boldsymbol{\omega}, \mathbf{n}_r) > 0,$$

where \mathbf{n}_r is the inner normal to the surface Γ at the point \mathbf{r} .

For us, it is of interest to consider the linear functionals found from solution of the transfer equation

$$J = \iiint_{R\Omega T} I(\mathbf{r}, \boldsymbol{\omega}, t) \varphi_D(\mathbf{r}, \boldsymbol{\omega}, t) d\mathbf{r} d\boldsymbol{\omega} dt. \quad (14)$$

Here R, Ω , and T refer to the subspace of eight-dimensional phase space $X = R \times \Omega \times T \times \Lambda$. Thus, $\mathbf{r} \in R, \boldsymbol{\omega} \in \Omega, t \in T$; φ_D is the weighting function, which in the simplest case has the following form (see Ref. 14)

$$\varphi_D(\mathbf{r}, \boldsymbol{\omega}, t, \lambda) = \delta(t - t^*) \delta(\mathbf{r} - \mathbf{r}^*) \Delta_{\Omega}(\boldsymbol{\omega}), \quad (15)$$

where t^* is the time of photon's entering some specified area of the phase space $\mathbf{r}^* \in D \subset R$, for example, the area of physical detector; Δ_Ω is the indicator function of the area $\omega \in D \subset \Omega$.

When the area D is small (what is typical of the situations in remote sensing), the sought functionals (14) are calculated with the help of the weighting modifications of the Monte Carlo method, most preferable among which are such approaches as the differential (local) flux estimate.^{14,15} Formally, the first order local estimate is determined as an analytical expression for the probability density of stochastic event, the latter implying that a photon after the n th ($n = 0, 1, 2, \dots$) state of the Markovian random walk chain enters the given area of the detector $D \subset X$:

$$J = \mathbf{E}\xi_1, \quad \xi_1 = \sum_{n=0}^N q_n h_1(\mathbf{x}_n \rightarrow \mathbf{x}^*) \delta\left(t_n + \frac{|\mathbf{r}_n - \mathbf{r}^*|}{v} - t\right), \quad (16)$$

where \mathbf{E} is the symbol of mathematical expectation, $\mathbf{x}_n = (\mathbf{r}_n, \omega_n, t_n)$; \mathbf{r}_n , ω_n , and t_n are the phase coordinates of the photon in the n th state of the Markovian chain, $\mathbf{x}^* \in D$; q_n are the photon statistical weights (Ref. 14); $h_1(\mathbf{x}_n \rightarrow \mathbf{x}^*)$ is the transition probability of the Markovian chain.

The form $h_1(\mathbf{x}_n \rightarrow \mathbf{x}^*)$ almost coincides (see Ref. 14) with the kernel of the original transfer equation rearranged to the integral form.

Thus, though the Monte Carlo method is not directly connected with the solution of integro-differential equation (12), however, constructing the effective weighting estimates, such as in Eq. (16), requires formal grounding.

The most general formalism of the transformation of a single-speed transfer equation to the integral Fredholm equation of the second kind are considered in Ref. 16 and generalized, for the case of multigroup theory, in Ref. 12. The integral transfer equation involving time dependence of the estimated functionals have been first formulated in Refs. 15 and 17 and later in Ref. 18.

Indeed, Eq. (12) can be presented in the operator form:

$$\mathbf{L}I = \mathbf{K}I + \frac{I_0}{\sigma(\mathbf{r})}, \quad (17)$$

where \mathbf{L} is the generalized operator of the differential transfer and \mathbf{K} is the integral operator of scattering.

Therefore,

$$I = (\mathbf{L}^{-1} \cdot \mathbf{K})I + \mathbf{L}^{-1}\left(\frac{I_0}{\sigma(\mathbf{r})}\right). \quad (18)$$

The technique of building up the complex operator $(\mathbf{L}^{-1} \cdot \mathbf{K})$ has been discussed in Ref. 16. Using this technique and omitting cumbersome computations we obtain the expression

$$I(\mathbf{r}, \omega, t) = \int_R d\mathbf{r}' \int_\Omega d\omega' \int_T dt' \frac{\sigma_s(\mathbf{r}')g(t')I(\mathbf{r}', \omega', t')}{2\pi|\mathbf{r} - \mathbf{r}'|^2 \sigma(\mathbf{r}')} \times \\ \times \exp\left[-\int_0^{|\mathbf{r}-\mathbf{r}'|} \sigma(\mathbf{r}'')d\mathbf{r}''\right] \delta\left(\omega - \frac{\mathbf{r} - \mathbf{r}'}{|\mathbf{r} - \mathbf{r}'|}\right) \times \\ \times \delta\left[t' - \left(t + \frac{|\mathbf{r} - \mathbf{r}'|}{v}\right)\right] + \Psi(\mathbf{r}, \omega, t), \quad (19)$$

where $\mathbf{r}' = \mathbf{r} - \omega l$, $0 \leq l \leq \xi^*$, ξ^* is the distance from the point $\mathbf{r} = (x, y, z)$ to the surface Γ along the direction ω ; $\Psi(\mathbf{r}, \omega, t)$ is the modified source function.

It is evident that in the generalized form Eq. (19) does not differ from its canonical variant

$$f(\mathbf{x}) = \int_X k(\mathbf{x}', \mathbf{x})f(\mathbf{x}')d\mathbf{x}' + f_0(x), \quad (20)$$

where $f(\mathbf{x}) = \sigma(\mathbf{r})I(\mathbf{x})$ is the photon collision density, $\mathbf{x} = \mathbf{x}(\mathbf{r}, \omega, t) \in X$.

Convergence of the Eq. (20) in the form of the Neumann series over collisions, under condition that

$$\|\mathbf{K}\| \leq \sup_x \int_X |k(\mathbf{x}', \mathbf{x})|d\mathbf{x}' < 1 \quad (21)$$

has been proved many times (see, e.g., Refs. 13 and 14).

It now follows from Eq. (19) that

$$h_1(\mathbf{x}_n \rightarrow \mathbf{x}^*) = \\ = \frac{\sigma_s(\mathbf{r}')g(\mu^*, t_j)\exp[-\tau(\mathbf{r}, \mathbf{r}^*)]}{\sigma(\mathbf{r}') \cdot 2\pi|\mathbf{r} - \mathbf{r}^*|^2 p(\mathbf{r}^*)} \Delta_\Omega(l^*)\Delta_i(t^*), \quad (22)$$

where $\Delta_\Omega(l^*)$ is the indicator of the detector area,

$l^* = \frac{\mathbf{r} - \mathbf{r}^*}{|\mathbf{r} - \mathbf{r}^*|}$; $\Delta_i(t^*)$ is the characteristic function of the

i th time interval of photon's occurrence in the

detector area; $\tau(\mathbf{r}, \mathbf{r}^*) = \int_0^{l^*} \sigma(\mathbf{r}(l))dl$ is the optical

length of the segment $[\mathbf{r}, \mathbf{r}^*]$; t_j stands for the time stages of the shape transformations of the scattering phase function, in this case $j = 1, 2, 3, 4$; $p(\mathbf{r}^*)$ is the distribution density of the random point $\mathbf{r}^* \in D \subset R$ over the detector volume. In this example, the selection of $p(\mathbf{r}^*)$ is not realized since the detector is positioned beyond the scattering volume. Thus, finiteness of the variance estimate by Eq. (16) is guaranteed.

Therefore, the local estimate by Eq. (22) also keeps canonical¹³⁻¹⁵ with the only exception that the scattering phase function assumes a discrete set of realizations conditioned by the physics of the process (see Fig. 3). The probability of choosing this or that form of $g(\mu)$ is governed by an *a priori* estimate of the portion of light energy scattered at each stage of $g(\mu)$ transformation.

We shall not consider particular algorithms of random selection determining photon trajectory, because these are well known (see, for example, Refs. 13–15, 17).

4. Numerical example

Below, we estimate the possible effect of the non-stationary kernel of the integral transfer equation onto the characteristics of multiply scattered pulsed radiation field. The calculations are done by the Monte Carlo method. These results are regarded as preliminary, because they are obtained for a particular case of a homogeneous monodisperse liquid-droplet medium with the particles of 5 μm radius. The boundary conditions reflect the possible scheme of lidar sensing of clouds.

A monochromatic light beam with the wavelength $\lambda = 0.8 \mu\text{m}$ and the divergence angle $\varphi_i = 0.5 \text{ mrad}$ is incident on the scattering layer of a certain specified optical thickness. The temporal and spatial profiles of the optical signal are set by the Gaussian functions according to Eq. (2) with $t_p = 50 \text{ fs}$ and $w_0 = 0.005 \text{ m}$. The functionals of interest (14) are the spatiotemporal intensity distributions of diffusely reflected and transmitted radiation in the neighborhood of the light beam.

The leading specialists in femtosecond atmospheric optics have expressed, in one of their recent paper,¹⁹ the idea of using spatioangular configuration of the field of multiply scattered radiation in the receiving plane of a monostatic sounding scheme for quality estimates of the cloud droplet spectrum. In this

connection, in Fig. 4 we present examples of angular distribution of diffusely backscattered and diffusely transmitted fluxes for point detector and flat one of 5-m radius. The estimates are given for integral over time fluxes. The results are compared to the standard stationary scattering phase function (classical Mie scattering⁶). It is characteristic that taking into account the non-stationary dependence $g(\mu, t)$, the geometric configuration of the angular distribution $I(\varphi_d)$ does not change too much, and in the case of a wide-angle reception, $\varphi_d \geq 0.04 \text{ rad}$, the dependence $g(t)$ does not manifest itself. At the same time, the integral values of backscattered and transmitted fluxes differ considerably: the portion of diffusely backscattered radiation grows and that of transmitted radiation drops.

Figure 5 illustrates the calculated time characteristic of the intensities of backscattered (*a*) and transmitted (*b*) signals.

Fourier method combined with the linear Mie theory.

The time behavior is expressed in the units of free photon path for different angular apertures of the point detector, $1/2\varphi_d = 0.5\text{--}175 \text{ mrad}$. The control results shown by curves 1–4 have been calculated using the classical stationary Mie scattering. Comparison of the results makes it possible to estimate the influence of shape transformation of the scattering phase function (great anisotropy decrease) onto the behavior and strength of backscattered and transmitted signals. The calculations have a local character, since they have been done for a monodisperse medium and for some values of pulse duration and droplet size.

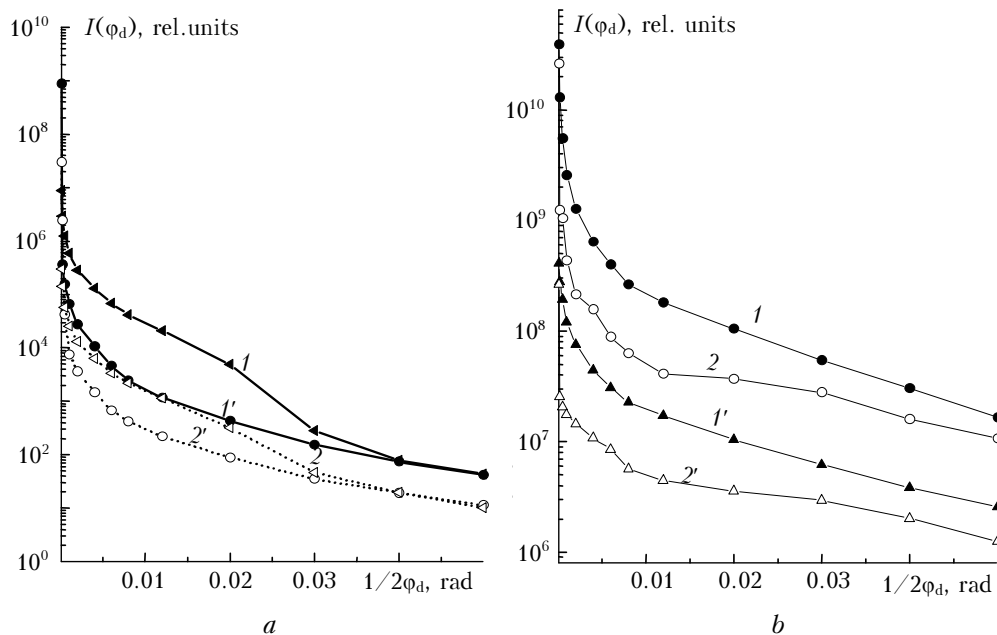


Fig. 4. Angular distribution of the integral flux of diffusely backscattered (*a*) and transmitted (*b*) radiation neglecting (curves 1, 2) and with the account of (curves 1', 2') the resonance interaction between femtosecond pulse and water droplets; 1, 1' refer to the point detector; 2, 2' refer to the flat detector (with a 5-m radius); optical depth of the layer is $\tau = 1.0$.

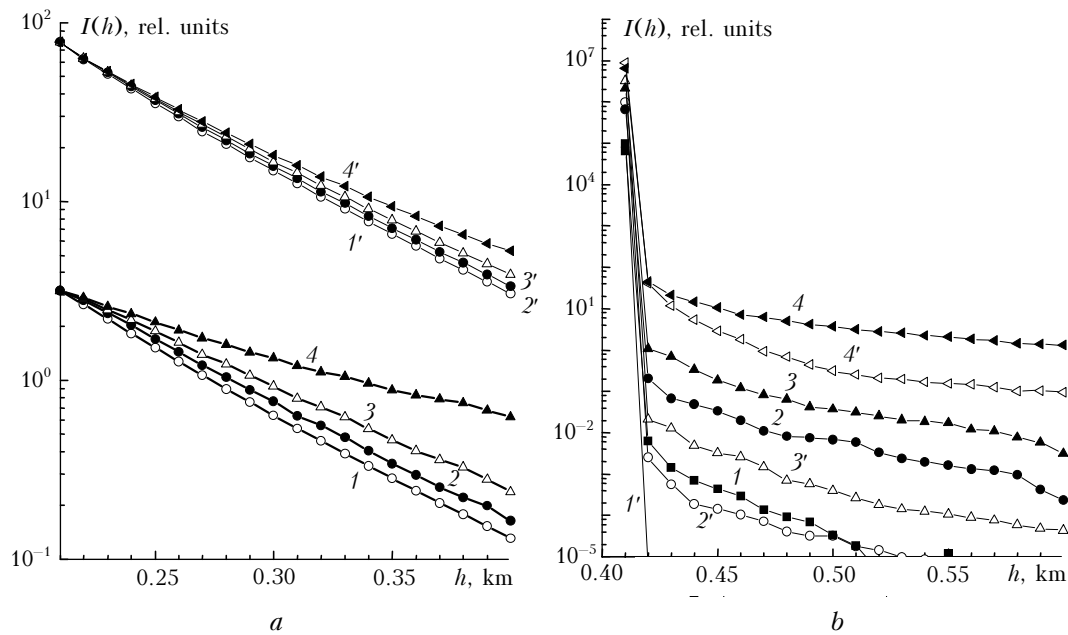


Fig. 5. Time distribution of the intensity of backscattered (*a*) and transmitted (*b*) signals depending on the angular receiving aperture with the account of (curves 1'–4') and neglecting (curves 1–4) the resonance pulse–droplet interaction; $\tau = 1.0$.

This circumstance does not enable making quantitative forecasts. However, the presence of noticeable growth of scattered radiation about the location angles, when the pulse duration is comparable to droplet sizes, is undoubtedly evident.

Conclusion

In this paper, we have proposed an analytical model of the nonstationary and inhomogeneous optical diffraction on a dielectric sphere. The model is based on the Fourier method combined with the linear Mie theory.

The obtained compact mathematical expressions allow a quantitative estimate of the characteristics of the nonstationary elastic scattering of ultra-short laser pulses by a water droplet, with its size being comparable to pulse length. Discovered is a notable transformation of the angular scattering function when the pulse goes through the droplet volume. These estimates were used as the input parameters for numerical solution of the integral transfer equation with a nonstationary kernel. The boundary conditions correspond to a typical scheme of laser sensing of clouds.

Preliminary results demonstrate the possibility of a considerable enhancement of the backscattering signal due to the reduction of anisotropy of the scattering phase function of a cloud droplet.

In the future, we are planning to estimate the effect of medium polydispersity and absorption by dielectric particles.

The results of this work were discussed at the 12th International Symposium on *Atmospheric and Ocean Optics. Atmospheric Physics* held in Tomsk in 2005 (Ref. 20).

Acknowledgments

The work is accomplished under the financial support of the Russian Foundation for Basic Research (grant No. 06–05–64799–a).

References

1. R. Fuchs and K.L. Kliewer, *J. Opt. Soc. Am.* **58**, No. 3, 319–330 (1968).
2. P. Chýlek, J.T. Kiehl, and M.K.W. Ko, *Appl. Opt.* **17**, No. 19, 3019–3021 (1978).
3. D.Q. Chowdhury, S.C. Hill, and P.W. Barber, *J. Opt. Soc. Am. B* **9**, No. 8, 1364–1373 (1992).
4. K.S. Shifrin and I.G. Zolotov, *Appl. Opt.* **34**, No. 3, 552–558 (1995).
5. A.A. Zemlyanov and Yu.E. Geints, *Opt. Spektrosk.* **96**, No. 2, 337–344 (2004).
6. C. Bohren and D. Huffman, *Absorption and Scattering of Light by Small Particles* (John Wiley & Sons Inc., New York–Chichester–Brisbane–Toronto–Singapore, 1983).
7. G. Gouesbet, B. Maheu, and G. Gréhan, *J. Opt. Soc. Am. A* **5**, No. 9, 1427–1443 (1988).
8. G. Gouesbet, G. Gréhan, and B. Maheu, *J. Opt. Soc. Am. A* **7**, No. 7, 998–1007 (1990).
9. J.A. Lock and G. Gouesbet, *J. Opt. Soc. Am. A* **11**, No. 9, 2503–2515 (1994).
10. A.A. Zemlyanov and Yu.E. Geints, *Atmos. Oceanic Opt.* **13**, No. 5, 412–422 (2000).
11. G.M. Krekov, M.M. Krekova, and S.S. Khmelevtsov, in: *Optical Propagation in the Atmosphere*, Collected papers (Nauka, Novosibirsk, 1975), pp. 34–47.
12. U. Fano, L. Spenser, and M. Berger, *Gamma-Radiation Transfer* (Gosatomizdat, Moscow, 1963), 284 pp.
13. G.I. Marchuk, ed., *Monte Carlo Method in Atmospheric Optics* (Nauka, Novosibirsk, 1976), 283 pp.
14. G.A. Mikhailov, *Optimization of Monte Carlo Weighting Methods* (Nauka, Moscow, 1987), 239 pp.

15. G.M. Krekov, G.A. Mikhailov, and B.A. Kargin, *Izv. Vyssh. Uchebn. Zaved. Fizika*, No. 9, 110–115 (1968).
16. V.S. Vladimirov, *Mathematical Problems of Single-speed Transfer Theory* (USSR Academy of Sciences Press, Moscow, 1961), 157 pp.
17. B.A. Kargin, in: *Probability Methods of Solving the Problems of Mathematical Physics* (Publishing House of CC SB AS USSR, Novosibirsk, 1971), 123–155 pp.
18. Z.M. Tan and P.F. Hsu, *J. Quant. Spectrosc. Radiat. Transfer* **73**, Nos. 2–5, 181–194 (2002).
19. R. Bourayon, G. Mejean, and Kosparian, *J. Opt. Soc. Am.* **22**, No. 2, 369–377 (2005).
20. Yu.E. Geints, A.A. Zemlyanov, G.M. Krekov, M.M. Krekova, and G.G. Matvienko, in: *Abstracts of Reports at XII Joint Int. Symp. on Atmospheric and Ocean Optics. Atmospheric Physics*, Tomsk (2005), p. 78.